Investigation of Combination of Finite Element Formulation and Element Type on the Accuracy of 3D Modeling of Polymeric Fluid Flow in an Extrusion Die

H. Sobhani, M. Razavi-Nouri, M. H. R. Ghoreishy

Department of Polymer Processing, Iran Polymer and Petrochemical Institute, PO Box 14965/115, Tehran, Iran

Received 28 September 2010; accepted 20 February 2010
DOI 10.1002/app.33394
Published online 1 December 2010 in Wiley Online Library (wileyonlinelibrary.com).

ABSTRACT: The aim of this work is to investigate the effect of finite element formulation and element type on the accuracy of 3D modeling of generalized Newtonian fluid flow in complex domains. Computer models based on three finite element solution schemes (mixed, continuous, and discrete penalty), and two element types (hexahedral and tetrahedral) in a 3D framework were developed. The well-known Carreau model was used to reflect the rheological behavior of the fluid. To determine the validity of the developed computer simulations, the flow of two high-density polyethylene (HDPE) melts with different viscosities through an extrusion die was simulated and compared with experimentally measured data. Comparison showed that the three methods produced nearly the same results with the hexahedral elements. However, continuous penalty method using tetrahedral elements demonstrated an extreme discrepancy from the experimental data. Discrete penalty method was unable to predict secondary variable (pressure) accurately using tetrahedral elements. The best results were obtained by the use of mixed method in conjunction with tetrahedral elements. © 2010 Wiley Periodicals, Inc. J Appl Polym Sci 120: 1607–1615, 2011

Key words: finite element method; penalty method; mixed method; generalized Newtonian; extrusion die

INTRODUCTION

It is quite well-known that the use of robust numerical technique for simulation of the polymer processing operation is inevitable. This is due to the nonlinearity of the governing equations and also the complex geometries that are normally required to form the polymer melt into final desired shape. There are different numerical methods that are usually used such as finite difference, finite element, finite volume, and boundary element schemes. However, owing to the greater flexibility in modeling of complicated geometries and ability to use highly accurate approximating approaches, finite element method is generally accepted as the best choice for this purpose. In addition, various types of boundary conditions can also be applied with the minimum level of mathematical efforts. The main difficulty associated with the application of finite element method for the fluid flow problems is incompressibility condition, which is imposed by the continuity equation. On the other hand, not only the pressure term is not included in continuity equation but also its interpolation functions should be one order less differentiable than the velocity components in momentum equations. Therefore, three submethods have been developed so far to tackle this problem, which are called as mixed or U-V-P,[1–4] continuous penalty,[5–9] and discrete penalty[10,11] methods. These techniques have widely been used to numerically simulate the different flow domains of polymer processes.

Although any combination of finite element formulation and element type can virtually be carried out, the predicted results are not in the same order of reliability and accuracy. Consequently, choosing a proper element and finite element scheme, especially for the 3D incompressible flow problems is the most important subject in this area because of its impact on computational cost and efforts and also on the accuracy and reliability of results. Most of the published works in this subject are based on the use of the incomplete elements (quadrilateral for 2D and hexagonal elements for 3D problems) as the development of their finite element working equations are more straightforward than the complete elements such as triangular and tetrahedral elements. However, our numerical experiments show that the hexagonal elements normally fail to discretize intricate 3D flow domains, which are generally encountered in industrial polymer processing problems. In most cases, tetrahedral elements are alternative selections, which can be used successfully to create finite element mesh.

Correspondence to: M. H. R. Ghoreishy (M.H.R.Ghoreishy@ippi.ac.ir).

The aim of this work is to study the effect of the combination of three above-mentioned finite element schemes (mixed, continuous, and discrete penalty) with two different element types (hexahedral and tetrahedral) on the accuracy of results obtained from numerical simulation of polymer melts in a typical pressure flow problem. The mathematical models were developed based on the solution of the continuity and momentum equations in 3D Cartesian framework. Two types of hexahedral and tetrahedral elements belonging to Taylor–Hood family[12,13] were used in this work. The well-known Carreau equation was also used to reflect the rheological behavior of polymer melts. The main assumptions made in the development of the present models are: (i) the flow of polymer is laminar and the fluid is incompressible; (ii) the flow is considered to be in a 3D Cartesian framework; (iii) body forces are negligible; and (iv) the flow regime is steady state and isothermal.

To examine the validity of the selected approaches, the flow of two polyethylene (PE) melts through an extrusion die were compared with experimentally measured pressure values and output mass flow rate. The main justification that leads us to assume isothermal system was based on the experimentally measured temperature profile in the longitudinal direction. It is shown that the maximum temperature rise was about 1°C. Furthermore, our numerical calculation confirmed that the temperature rising in the longitudinal direction of die is negligible. In addition, it should be noted that our main goal was to examine the numerical effectiveness of the developed algorithms. Therefore, any nonisothermal solution method can easily be joined with the selected method.

In the following sections, we first describe the mathematical model and then the finite element working equations are briefly introduced. The simulation results and comparison of them with experimental data are presented in the next section and finally conclusions are drawn.

MATHEMATICAL MODEL

The governing equations of the flow of an incompressible generalized Newtonian fluid in a 3D Cartesian coordinate system in the absence of body force are given as[14]:

1. The continuity equation:

$$\nabla \cdot \underline{v} = 0 \tag{1}$$

2. The momentum equation:

$$\rho \frac{D\underline{v}}{Dt} = -\nabla p + \nabla \cdot \underline{\underline{\tau}} \tag{2}$$

In these equations, $\underline{v}$ is the velocity vector, p is the pressure, ρ is the material density, and $\underline{\underline{\tau}}$ is the viscose stress tensor which is given for a generalized Newtonian fluid in terms of rate-of-deformation tensor $\underline{\underline{\Delta}}$ by:

$$\underline{\underline{\tau}} = \eta \underline{\underline{\Delta}} \tag{3}$$

where η is shear-dependent non-Newtonian viscosity of the fluid. The rate-of-deformation tensor is defined as:

$$\underline{\underline{\Delta}} = \nabla \underline{v} + (\nabla \underline{v})^T \tag{4}$$

Viscosity (η) in this study is selected to be described by the Carreau model[14]:

$$\frac{\eta - \eta_\infty}{\eta_0 - \eta_\infty} = \left[1 + \lambda_0^2 \left(\frac{1}{2} I_2\right)\right]^{\left(\frac{n-1}{2}\right)} e^{-b(T-T_0)} \tag{5}$$

where η_0 and η_8 are constant viscosity at zero and infinite shear rate, respectively, λ_0 is a material time constant known as relaxation time, n is the power-law index, T_0 is a reference temperature, b is the temperature sensitivity coefficient, and I_2 is the second invariant of the rate-of-deformation tensor defined as:

$$I_2 = \underline{\underline{\Delta}} : \underline{\underline{\Delta}} \tag{6}$$

FINITE ELEMENT FORMULATIONS

As it is mentioned earlier, three finite element schemes (mixed, continuous, and discrete penalty) have been used in this work. Details of the working equations of each method can be found in a number of references.[6,7,12,13] Consequently, in this section only a brief description of each technique will be presented.

Mixed method

In this method, both velocity and pressure are regarded as primitive variables and discretized. The most necessary requirement in the application of the mixed method is the satisfaction of stability known as the Ladyzhenskaya–Babuska–Brezzi (LBB) condition.[12,15] This requirement arises from the absence of the pressure in continuity equation and also one order less differentiation of the pressure than velocity components in momentum equations. It has been found that the mixed method in conjunction with elements generating equal interpolations for velocity and pressure yield inaccurate and oscillatory results. These oscillations can be disappeared by the use of elements of Taylor–Hood or Crouzeix–Raviart family.[13–14,16] We have used tetrahedral and hexahedral elements belonging to the Taylor–Hood

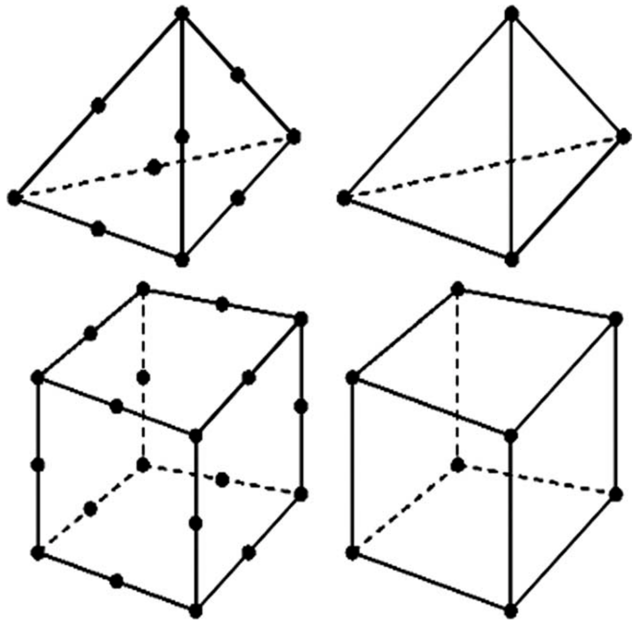

Figure 1 Tetrahedral and hexahedral elements belonging to Taylor–Hood family elements; right-hand elements are for pressure and left-hand elements are for velocity.

family in this study to satisfy LBB condition (Fig. 1). In these elements, the velocity and pressure fields are approximated using biquadratic and bilinear shape functions, respectively, thus providing unequal order of interpolations for velocities and pressure.

Penalty formulation

The penalty formulation allows the elimination of the pressure variable in the momentum equations using:

$$p = -\lambda(\nabla \cdot \underline{v}) \tag{7}$$

where λ is a large number (in order of 10^8–10^{12}) known as penalty parameter. It can be shown that if we choose λ to be a relatively large enough, the continuity equation will be satisfied. To enforce the continuity at the right level in the non-Newtonian flow problems, where shear-dependent viscosity varies locally, it is necessary to maintain a balance between the viscosity and the penalty parameter. Therefore, λ should be expressed as a function of viscosity, and eq. (7) is then written as:[17]

$$p = -\lambda^*(\nabla \cdot \underline{v}) \tag{8}$$

where

$$\lambda^* = \eta\lambda \tag{9}$$

There are two schemes for the implementation of the penalty relation to eliminate the pressure terms in momentum equations. These are known as the continuous and discrete penalty technique. This is because that the elimination of the pressure variable from momentum equations dose not yield a robust scheme for incompressible flow, and it is necessary to satisfy the LBB stability condition by a suitable technique.[12,13,17]

Continuous penalty method

In this method, the pressure in the momentum equations is directly substituted from the penalty relation [eq. (8)]. The obtained equations are then discretized using the traditional Galerkin finite element approach. However, to achieve a nontrivial solution and satisfaction of the LBB stability condition, the penalty terms in the stiffness matrix coefficients must be evaluated using a reduced integration method.[13,17] In this study, standard tetrahedral and hexahedral elements with 10 and 20 nods, respectively, were used for calculating velocity and pressure.[13,15] In these elements, velocity and pressure are approximated using biquadratic shape functions. It is also found that the best results are achieved using continuous penalty scheme when λ is equal to 10^{10}.

Discrete penalty method

In the discrete penalty method, the pressure term in momentum equations is substituted by the discretized form of the modified continuity equation.[13,17] To satisfy the LBB stability condition, appropriate interpolation relations have to be selected for velocity and pressure. Therefore, in this work, tetrahedral and hexahedral elements belonging to the Taylor–Hood family similar to mixed method were used to achieve this task. The working equations of discrete penalty method are derived using Galerkin method. Based on numerical trial and error, the best results for discrete penalty method was achieved choosing λ to be equal to 10^7.

Pressure is unknown in the mixed finite element approach while the continuous penalty method allows its elimination and thus the size of the global matrix is considerably reduced. The discrete method combines the advantages of computational economy with the robustness of a numerical scheme in which the LBB condition is directly satisfied.

Secondary calculations and boundary conditions

The pressure field in both penalty methods (continuous and discrete) is generally found by a secondary calculation such as the variational recovery method.[15] To complete mathematical models, the governing equations must be solved in conjunction with the appropriate set of boundary conditions. For

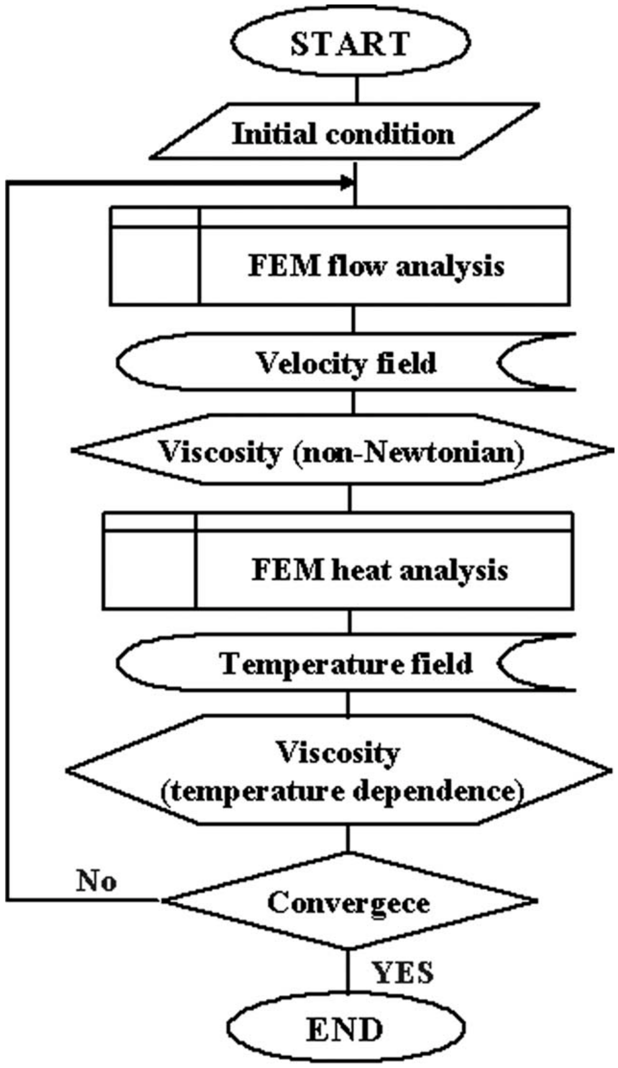

Figure 2 Flow diagram of nonisothermal flow analysis.

the inlet of flow domain, average velocity and the no-slip condition on the solid walls which are the first-type boundary condition are used. For the outlet, pressure and stress-free conditions which are the second-type boundary condition are specified.

Isothermal assumption

The energy equation of the flow of an incompressible generalized Newtonian fluid in a 3D Cartesian coordinate system is given as[14]:

$$\rho c_p\left(\frac{\partial T}{\partial t}+\underline{\mathrm{v}}\cdot\nabla T\right)=\nabla\cdot k\nabla T+2\eta D:D \qquad (10)$$

In this equation, $\underline{\mathrm{v}}$ is the velocity vector, p is the pressure, T is the temperature, ρ is the material density, c_p is the heat capacity of polymer melt, k is the thermal conductivity of polymer melt, and η is shear-dependent non-Newtonian viscosity of the fluid.

The use of standard Galerkin finite element method for the solution of the convection dominated equations encountered in polymer processing operations such as the energy equation normally gives unstable and oscillatory results. These oscillations disappeared by the use of the streamline upwinding scheme. In this scheme, different weight functions are used for convection and the other terms in energy equations.[12,15] Details of the working equations of this method can be found in a number of references.[7,13] Figure 2 represents the flow diagram for the nonisothermal simulation applied in this study. Our calculation indicated that the temperature rise in the longitudinal direction is negligible. Figure 3 shows the temperature distribution for a sample of the simulated materials at the screw speed of 60 rpm. As it can be seen in this figure, the maximum temperature difference between inlet and outlet of the die is 1.4°C. Consequently, the isothermal assumption in this work is fully justified. Therefore, there is no need to include the nonisothermal equations in the numerical scheme.

SOLUTION STRATEGY

Having used the well-known isoparametric mapping, the working equations of the different schemes are cast into local natural coordinate system. The members of the submatrix and subvector are then computed for each element by appropriate Gauss quadrature method. The resulting algebraic equations are assembled into a global matrix and solved by a frontal solution algorithm[18] after imposing the appropriate set of boundary conditions. The presence of the convective terms in the momentum equations and also dependency of the viscosity on velocity gradient make the final set of assembled

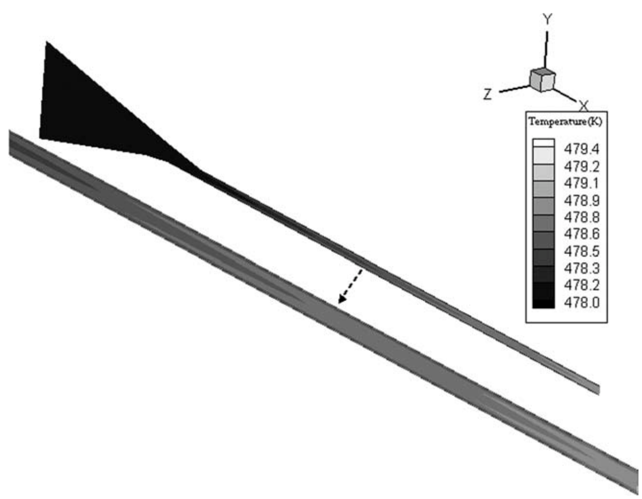

Figure 3 Temperature distribution at screw speed of 60 rpm for LV-HDPE.

TABLE I
Physical and Rheological Properties of the Two PE Melts

Properties	PE-5218	PE-EX3
Code	LV-HDPE	HV-HDPE
Power-law index (n)	0.85	0.29
η_0 (Pa s^n)	1130	56,600
λ (s)	0.95	0.92
Melt density, ρ (kg/m^3)	760	780
Melt Flow Index (MFI) (g/10 min)	17–19	0.4–0.7

equations nonlinear. Therefore in this work, the Picard's iterative procedure is used to handle the nonlinear nature of the derived equations. The convergence criterion used in this work is given by;

$$\sqrt{\frac{\sum_{j=1}^{N}\left|X_j^{r+1}-X_j^{r}\right|^2}{\sum_{j=1}^{N}\left|X_j^{r+1}\right|^2}} \leq \delta \qquad (11)$$

where X_j^r denotes the field components (velocity or pressure) corresponding to the degree of freedom j at iteration cycle r, and δ is the convergence to tolerance (say, 10^{-3}).

RESULTS AND DISCUSSION

Based on the above-described methods and algorithms, a computer code was developed in FORTRAN. Preprocessing and postprocessing steps in this work were performed using an interactive commercial package called GEOSTAR.[19] For the investigation of the effect of viscosity on the performance of models, two grades of high-density PE (HDPE) with different melt indices were used. These HDPEs were supplied by Tabriz Petrochemical Co. and Tabriz/Iran and Amir Kabir Petrochemical Co., Mahshahr/Iran with the trade names of HDPE-5218 and HDPE-EX3, respectively. Table I shows the physical and rheological properties of the materials used. The rheological properties of these HDPEs were measured using capillary rheometer (Instron, model 3211) at 190°C. The rheological parameters of the HDPE melts were calculated using the Carreau rheological model. The flow of these HDPE melts through the die region of a single screw extruder was simulated by the use of the mentioned computer code. To verify the accuracy of various elements and methods as well as the numerical algorithms, the simulation results were compared with the experimental runs on a laboratory extruder (Brabender). Figure 4 illustrates the extruder and the geometry of entrance of the die. Five screw speeds of 20, 40, 60, 80, and 100 rpm were selected in this experience. For each experiment, the pressures at three locations and also mass flow rate were measured. Figure 5 shows the flow domain and the applied boundary condition of the extrusion die as well as the locations of the pressure transducers. The temperature on solid wall and inlet region was set to be 190°C. For each simulation, the measured velocity computed by the division of the measured mass flow rate to the area of the inlet section was selected as the boundary condition. In addition to guaranty of obtaining converged and accurate results, two mesh configurations with different degrees of refinement were used. Specifications of these configurations are recorded in Table II. Figure 6(a and b) shows the mesh configuration II using the mentioned elements. Moreover, for both element types, higher order interpolation functions were also used. Table III gives the calculated and experimentally measured mass flow rates and pressure for low-viscosity HDPE (LV-HDPE; see Table I for code

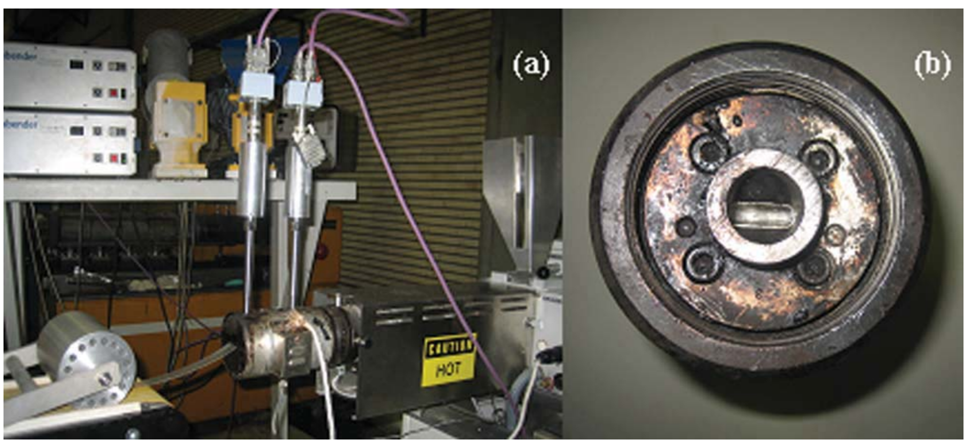

Figure 4 (a) Instruments setup applied for measuring pressures and mass flow rates and (b) entrance of the die. [Color figure can be viewed in the online issue, which is available at wileyonlinelibrary.com.]

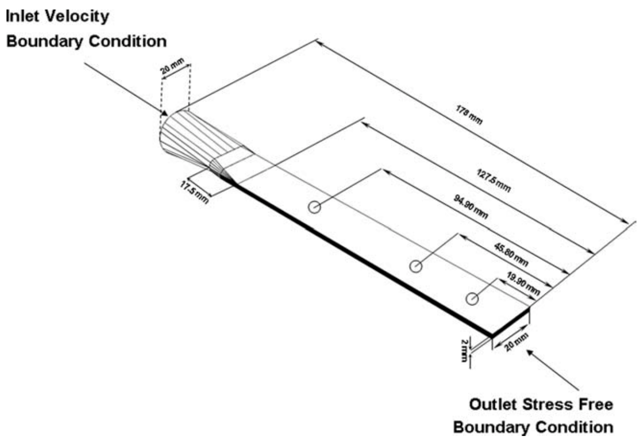

Figure 5 Flow domain with boundary condition.

TABLE II
Specification of the Finite Element Mesh

Configuration	Element type	Number of elements	Number of nodes
I_h	20-noded hexahedral	960	5073
II_h	20-noded hexahedral	1810	9312
I_t	10-noded hexahedral	6415	9785
II_t	10-noded hexahedral	8915	16,008

designation) at screw speed of 60 rpm using mixed method. It can be seen that the configuration II for tetrahedral and hexahedral elements gives converged results. Therefore, this configuration was selected for simulations.

The experimentally measured pressures at three zones and also the simulated pressure profiles through center line of the die corresponding to the screw speeds of 20, 40, and 60 rpm for LV-HDPE and 20 and 60 rpm for high-viscosity HDPE (HV-HDPE) using hexahedral elements with various methods are shown in Figures 7 and 8, respectively. As it can be seen, there is no significant difference between the results calculated by the three finite element methods with hexahedral elements. Table IV represents some selected results of the simulated and experimentally measured pressure and mass flow rates corresponding to each screw speed for the two HDPE grades using three finite element methods and hexahedral elements. It can be found that there are good agreements between the simulation and experimental results for both HDPEs grade. Therefore, the trivial differences between simulated mass flow rates and pressures with experimental data reveal that the mixed, continuous, and discrete penalty methods give nearly identical and accurate results using hexahedral elements. The discrepancies can be attributed to the nature of approximation associated with each numerical technique and also the error of the measuring of the pressures and mass flow rates. On the other hand, the die used in this research has been made of two main parts. The first part is a converging region, and second part has a simple slit geometry. Therefore, during the discretization process using hexahedral element, tip curves in converging region had to be eliminated. Owing to this simplifying step, the simulated pressures were found to be a little higher than that of the experimental data. However, this difference can be significant for more complex geometries and thus these elements cannot be used successfully for such domains.

In spite of the robustness and minor sensitivity of the hexahedral elements to the selected finite element method, its flexibility in creating the mesh for complex domains is low. This means that they are unable to correctly discretize curves and tip corners. To investigate the effect of element type on modeling, these simulations were repeated using tetrahedral elements. It is found that the results obtained using continuous penalty method with tetrahedral elements diverge extremely from the experimental

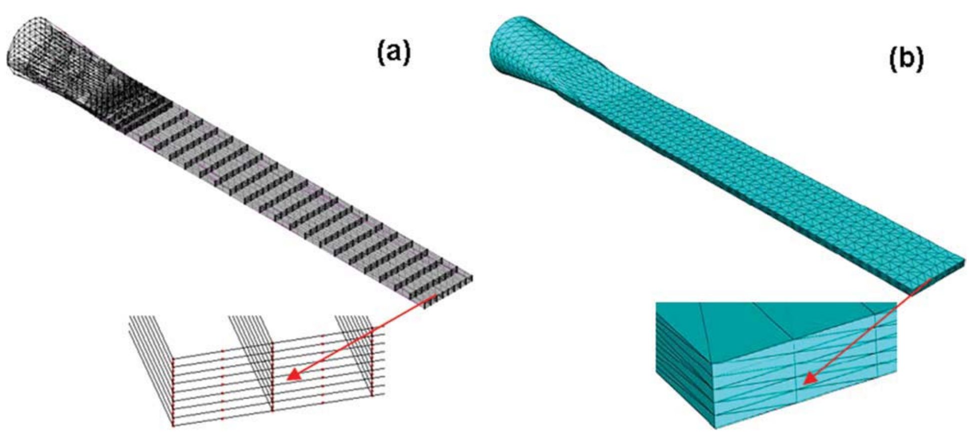

Figure 6 Finite element mesh (a) hexahedral (b) tetrahedral elements corresponding to mesh configuration II. [Color figure can be viewed in the online issue, which is available at wileyonlinelibrary.com.]

TABLE III
Simulated and Experimental Measured Results for LV-HDPE at Screw Speed of 60 rpm for Different Mesh Configurations

	Mass flow rate (g/s)		Pressure zone 1		Pressure zone 2		Pressure zone 3	
Mesh	Sim.	Exp.	Sim.	Exp.	Sim.	Exp.	Sim.	Exp.
I_h	1.152	1.138	6.50	6.65	2.98	3.15	1.31	1.42
II_h	1.143	1.138	6.58	6.65	3.20	3.15	1.45	1.42
I_t	1.149	1.138	6.54	6.65	3.03	3.15	1.34	1.42
II_h	1.140	1.138	6.62	6.65	3.13	3.15	1.40	1.42

data and thus this combination is not applicable for the simulation of flow problems. This is because that the proper choice of reduced integration points in Gauss quadrature for tetrahedral elements cannot be carried out as precisely as the case of the hexahedral elements. Table V represents the simulated and measured mass flow rates as well as pressures by mixed and discrete penalty methods using tetrahedral elements at different screw speeds. The results show that the differences in computed mass flow rates for these methods are negligible, and therefore these methods give converged results using tetrahedral elements.

However, comparison of the simulated and measured pressures for discrete penalty shows that the differences between these set of data are relatively high, and discrete penalty method is unable to accurately predict secondary variable in this case. This is due to the lack of sufficient accuracy in secondary calculations (variational recovery) with tetrahedral elements. Moreover, the definition of the accurate reduced Gauss points for tetrahedral elements cannot be accomplished in continuous penalty method and thus the continuity equation is not correctly satisfied. As it can be seen in Table V, the simulation results obtained using mixed method are relatively similar to measured pressures, and this confirms the validity of the mixed model. Moreover, as tetrahedral elements can completely mesh the complex geometries and it is not required to simplify the geometries, the results obtained by these elements are therefore more accurate than those predicted by the hexahedral elements. This can be confirmed by the comparison of the results of mixed method with hexahedral and tetrahedral elements as recorded in Tables IV and V, respectively.

The experimentally measured pressures at three zones and also the simulated pressure profile in center line of the die at various screw speeds for LV-HDPE and HV-HDPE are shown in Figures 9 and 10, respectively. As it can be observed, a very smoothed and nonoscillatory pressure profile has been obtained for each screw speed. This is due to the consistency of the interpolation functions selected for pressure and velocity for the 10-nodded tetrahedral elements in conjunction with a relatively refined mesh. Therefore, in spite of difficulty in considering the pressure variable in a pure pressure flow with mixed method, the predicted pressure profile reveals that this finite element technique along with tetrahedral elements can be used successfully to simulate the pressure flow in polymer processing operations.

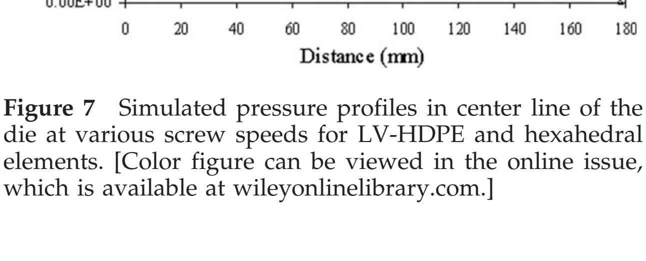

Figure 7 Simulated pressure profiles in center line of the die at various screw speeds for LV-HDPE and hexahedral elements. [Color figure can be viewed in the online issue, which is available at wileyonlinelibrary.com.]

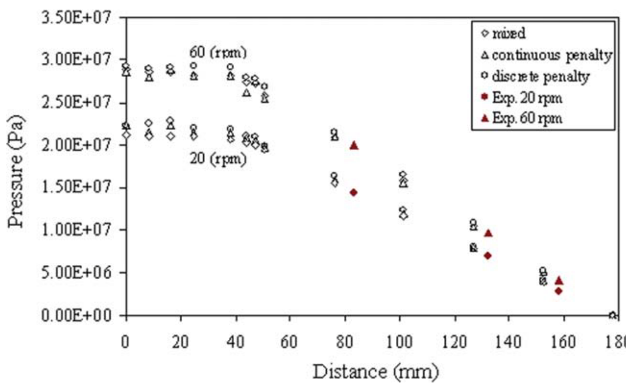

Figure 8 Simulated pressure profiles in center line of the die at various screw speeds for HV-HDPE and hexahedral elements. [Color figure can be viewed in the online issue, which is available at wileyonlinelibrary.com.]

TABLE IV
Experimental and Simulated Pressures and Mass Flow Rates for Hexahedral Elements

Finite element methods (FEMs)	Screw speed (rpm)	PE type	Mass flow rate (g/s)			Pressure zone 1			Pressure zone 2			Pressure zone 3		
			Sim.	Exp.	Err%	Sim.	Exp.	Err%	Sim.	Exp.	Err%	Sim.	Exp.	Err%
Mixed	20	LV-HDPE	0.22	0.222	0.9	1.47	1.45	1.38	0.72	0.71	1.41	0.31	0.3	3.33
		HV-HDPE	0.185	0.187	1.07	14.48	14.45	0.21	6.94	6.92	0.29	2.82	2.8	0.71
Continuous penalty	20	LV-HDPE	0.219	0.222	1.35	1.48	1.45	2.07	0.73	0.71	2.82	0.31	0.3	3.33
		HV-HDPE	0.184	0.187	1.6	14.49	14.45	0.28	6.94	6.92	0.29	2.83	2.8	1.07
Discrete penalty	20	LV-HDPE	0.224	0.222	0.9	1.5	1.45	3.45	0.74	0.71	4.23	0.31	0.3	3.33
		HV-HDPE	0.19	0.187	1.6	14.5	14.45	0.35	6.96	6.92	0.58	2.84	2.8	1.43
Mixed	60	LV-HDPE	0.653	0.658	0.76	3.99	3.95	1.01	1.89	1.86	1.61	0.91	0.89	2.25
		HV-HDPE	0.535	0.539	0.74	20.07	20	0.35	9.69	9.65	0.41	4.24	4.2	0.95
Continuous penalty	60	LV-HDPE	0.651	0.658	1.06	3.91	3.95	1.01	1.9	1.86	2.15	0.87	0.89	2.25
		HV-HDPE	0.533	0.539	1.11	20.04	20	0.2	9.62	9.65	0.31	4.23	4.2	0.71
Discrete penalty	60	LV-HDPE	0.663	0.658	0.76	3.92	3.95	0.76	1.9	1.86	2.15	0.92	0.89	3.37
		HV-HDPE	0.544	0.539	0.93	20.09	20	0.45	9.7	9.65	0.52	4.25	4.2	1.19
Mixed	100	LV-HDPE	1.143	1.138	0.44	6.58	6.65	1.05	3.2	3.15	1.59	1.45	1.42	2.11
		HV-HDPE	0.885	0.88	0.57	22.99	22.95	0.17	11.14	11.1	0.36	4.99	4.95	0.81
Continuous penalty	100	LV-HDPE	1.132	1.138	0.53	6.71	6.65	0.9	3.11	3.15	1.27	1.37	1.42	3.52
		HV-HDPE	0.875	0.88	0.57	22.9	22.95	0.22	11.15	11.1	0.45	5	4.95	1.01
Discrete penalty	100	LV-HDPE	1.144	1.138	0.53	6.59	6.65	0.9	3.1	3.15	1.59	1.38	1.42	2.82
		HV-HDPE	0.884	0.88	0.45	22.89	22.95	0.26	11.16	11.1	0.54	4.99	4.95	0.81

TABLE V
Experimental and Simulated Pressures and Mass Flow Rates for Tetrahedral Elements

Finite element methods (FEMs)	Screw speed (rpm)	PE type	Mass flow rate (g/s)			Pressure zone 1			Pressure zone 2			Pressure zone 3		
			Sim.	Exp.	Err%	Sim.	Exp.	Err%	Sim.	Exp.	Err%	Sim.	Exp.	Err%
Mixed	20	LV-HDPE	0.221	0.222	0.45	1.44	1.45	0.69	0.71	0.71	0	0.305	0.3	1.67
		HV-HDPE	0.186	0.187	0.53	14.47	14.45	0.14	6.93	6.92	0.14	2.79	2.8	0.36
Discrete penalty	20	LV-HDPE	0.224	0.222	0.9	N/A	1.45	N/A	N/A	0.71	N/A	N/A	0.3	N/A
		HV-HDPE	0.189	0.187	1.07	N/A	14.45	N/A	N/A	6.92	N/A	N/A	2.8	N/A
Mixed	60	LV-HDPE	0.655	0.658	0.46	3.93	3.95	0.51	1.85	1.86	1.61	0.9	0.89	1.12
		HV-HDPE	0.537	0.539	0.37	19.97	20	0.15	9.63	9.65	0.1	4.18	4.2	0.48
Discrete penalty	60	LV-HDPE	0.662	0.658	0.61	N/A	3.95	N/A	N/A	1.86	N/A	N/A	0.89	N/A
		HV-HDPE	0.542	0.539	0.56	N/A	20	N/A	N/A	9.65	N/A	N/A	4.2	N/A
Mixed	100	LV-HDPE	1.14	1.138	0.18	6.62	6.65	0.45	3.13	3.15	0.63	1.4	1.42	1.41
		HV-HDPE	0.882	0.88	0.23	22.93	22.95	0.09	11.08	11.1	0.18	4.92	4.95	0.61
Discrete penalty	100	LV-HDPE	1.141	1.138	0.26	N/A	6.65	N/A	N/A	3.15	N/A	N/A	1.42	N/A
		HV-HDPE	0.884	0.88	0.45	N/A	22.95	N/A	N/A	11.1	N/A	N/A	4.95	N/A

N/A, The data simulated of these conditions are not presented due to the highly deviation from experimental measurements and also data calculated by other methods.

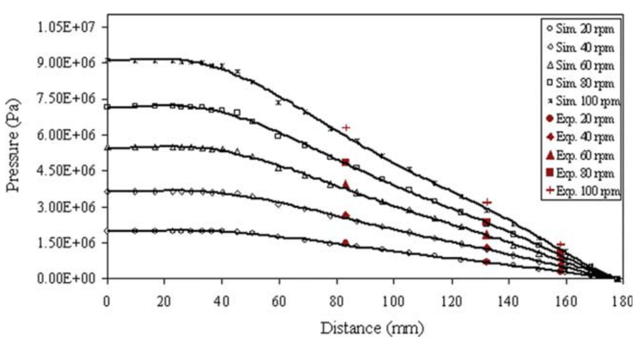

Figure 9 Simulated pressure profile in center line of the die at various screw speeds using mixed method and tetrahedral elements for LV-HDPE. [Color figure can be viewed in the online issue, which is available at wileyonlinelibrary.com.]

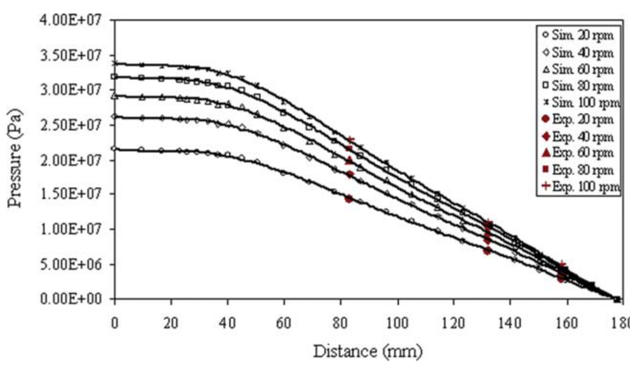

Figure 10 Simulated pressure profile in center line of the die at various screw speeds using mixed method and tetrahedral elements for HV-HDPE. [Color figure can be viewed in the online issue, which is available at wileyonlinelibrary.com.]

CONCLUSIONS

The flow of two HDPEs with different melt flow indices throughout an extruder die has been simulated using three different 3D finite element methods of mixed, continuous, and discrete penalty in conjunction with two types of hexahedral and tetrahedral elements. The validity of the developed models was investigated by comparison of the simulation results with experimentally measured data. It is found that the three finite element solution schemes in conjunction with hexahedral element provide high level of accuracy, and nearly identical results are obtained. However, the results obtained with tetrahedral element showed that this element cannot be used with continuous penalty method. In addition, discrete penalty technique fails to accurately predict the pressure profile with tetrahedral elements, although the comparison of the mass flow rates with experimental data confirmed the ability of this method for prediction of the mass flow rates. It is also found that hexahedral elements are unable to discretize highly complex geometries and thus their applicability in simulation is limited to simplified domains. On the other hand, the tetrahedral element can virtually be used to create finite element mesh for any geometry. Consequently, the combination of a mixed finite element technique for the derivation of the working equations with tetrahedral elements to discretize of the domain is the best choice for the simulation of the flow of polymer melts in complicated flow domains.

References

1. Zienkiewicz, O. C.; Wu, J. Int J Numer Methods Eng 1991, 32, 1189.
2. Heuveline, V. Int J Numer Methods Fluids 2003, 41, 1339.
3. Wong, J. C. F.; Yuan, P. Commun Numer Methods Eng 2007, 23, 983.
4. Bustinza, R.; Gatica, G. N.; Gonzalez, M. Int J Numer Methods Fluids 2005, 49, 877.
5. Ghoreishy, M. H. R.; Razavi-Nouri, M. Iran Polym J 1998, 7, 277.
6. Ghoreishy, M. H. R.; Razavi-Nouri, M. J Appl Polym Sci 1999, 74, 676.
7. Ghoreishy, M. H. R.; Razavi-Nouri, M.; Naderi, G. Comput Mater Sci 2005, 34, 389.
8. Jog, C. S. Int J Numer Methods Eng 2008, 73, 123.
9. Mu, Y.; Zhao G.; Qin, Sh.; Chen, A. Polym Adv Technol 2007, 18, 1004.
10. Yinnian, H. Math Comput 2005, 74, 1201.
11. Yuan, L.; Kaitai, L. Appl Math Comput 2008, 204, 216.
12. Donea, J.; Huerta, A. Finite Element Methods for Flow Problems; Wiley: Chichester, 2003.
13. Nassehi, V. Practical Aspects of Finite Element Modelling of Polymer Processing; Wiley: Chichester, 2002.
14. Bird, R. B.; Stewart, W. E.; Lightfoot, E. N. Transport Phenomena, 2nd ed.; Wiley: New York, 2002.
15. Zienkiewicz, O. C.; Taylor, R. L. Finite Element Method, Fluid Dynamics, 5th ed.; Butterworth-Heinemann: Oxford, 2000; Vol. 3.
16. Reddy, J. N.; Gartling, D. K. The Finite Element Method in Heat Transfer and Fluid Dynamics, 2nd ed.; CRC Press: New York, 2001.
17. Pittman, J. F. T. In Finite Element for Field Problems in Fundamentals of Computer Modeling for Polymer Processing; Tucker, C. L., III, Ed.; Hanser Publishers: Munich, 1989.
18. Hood, R. Int J Numer Methods Eng 1976, 10, 379.
19. COSMOS/M software, Command Reference, Structural Research and Analysis Corporation, Los Angeles, California, Version 2.85, 2003.